Different Radiation Impedance Models for Finite Porous Absorbers

Mélanie Nolan[1], Cheol-Ho Jeong, Jonas Brunskog
Acoustic Technology, Technical University of Denmark, 2800 Kgs. Lyngby, Denmark

Julia Rodenas, Fabien Chevillotte, Luc Jaouen
Matelys, 1 rue Baumer, 69120 Vaulx-en-Velin, France

Summary

The Sabine absorption coefficients of finite absorbers are measured in a reverberation chamber according to the international standard ISO 354. They vary with the specimen size essentially due to diffraction at the specimen edges, which can be seen as the radiation impedance differing from the infinite case. Thus, in order to predict the Sabine absorption coefficients of finite porous samples, one can incorporate models of the radiation impedance. In this study, different radiation impedance models are compared with two experimental examples. Thomasson's model is compared to Rhazi's method when coupled to the transfer matrix method (TMM). These methods are found to yield comparable results when predicting the Sabine absorption coefficients of finite porous materials. Discrepancies with measurement results can essentially be explained by the unbalance between grazing and non-grazing sound field in the reverberation chamber. A better agreement is found when incorporating the modal decomposition method to the models.

PACS no. 43.55.Ev, 43.55.Ka

1. Introduction

The radiation of sound from plane surfaces is of special importance for many problems concerning noise and vibration. One example is the calculation of the sound transmission coefficient of a finite wall. The sound absorption of finite surface areas is another example. The sound pressure is a field variable, which is calculated via Kirchhoff-Helmholtz equation. It is typically not the best measure for the radiated sound field, so that the radiated power is considered a better alternative. In all cases, the effect of the finiteness of the radiating surface must be included.

Cremer and Heckl [1, 2] derived a formula to calculate the power radiated from a structure using the spatial Fourier transform. As the transformed velocity is directly used in the formula, the inverse transform is not required in the solution, which is computationally efficient. The power radiated from any spatially transformed velocity can be calculated. In [2], Cremer and Heckl made use of the formula to study the effect of radiation from finite vibrating panels. The approach is based on the spatial windowing of a single plane structural wave so that the vibration velocity outside the finite area is zero.

In many applied situations, the radiation efficiency is used to calculate the radiated power. Based on the formula provided by Cremer and Heckl, Villot et al. [3] also studied the radiated power and the radiation efficiency of finite structures using the same spatial windowing technique of plane waves. They applied the method to multi-layered structures using the transfer matrix method.

The available techniques for determining the radiated power or radiated efficiency of a finite structure using spatial windowing of the formula suggested by Cremer and Heckl, have one common drawback in that the wave number spectrum is calculated directly for the case of radiation from a finite area, which is not the case in many practical applications.

An alternative approach is suggested by Atalla et al. [4], who considered the sound power radiation of planar surfaces using a Rayleigh-integral based method in connection with the transfer matrix method, in order to account for the effect of the finite size. The method is known under the name of finite transfer matrix method (FTMM). The transfer matrix method is used along with the same spatial windowing as in [3] but the numerical integration is eased by two changes of variables.

[1] Author to whom correspondence should be addressed

This approach is commonly used for prediction of the lateral size effects on the acoustic absorption. The calculation of the radiation impedance being computationally heavy, Rhazi et al. [5] suggested an analytical simplification that allows for a faster computation of the radiated power of multilayered panels. The radiation impedance used in the FTMM is found to be the same radiation impedance as the one developed earlier by Thomasson [6].

In the case of sound absorption of finite patches, Thomasson [6] has shown that the area dependence, and thereby the so called *edge-effect*, can be described with a specific radiation or field impedance which depends on the geometrical shape of the absorption patch and the incidence angles. He derived simple formulas for the area correction of the absorption coefficient using a variational approach.

The purpose of this paper is to compare the results of Rhazi et al. with those of Thomasson when predicting the random incidence absorption coefficient of finite porous materials. Porous absorbers mounted on a rigid wall and backed by a cavity are investigated. A short overview of the possible explanations for the disagreement between simulation results and measured data will be given and ways of improving the models suggested.

Although both models hold for extendedly reacting surfaces, Thomasson originally assumed that the wave transmitted into the porous material is refracted so that it propagates effectively only perpendicular to the surface. This is referred to as a locally reacting surface. The assumption of local reaction is widely used in room acoustic simulations, the main reason being its simplicity compared to non-local or extended reaction models. However, the adequacy of the assumption of local reaction is questionable for porous layers backed by an air cavity [7]. The present paper will show the effect of incorporating extended reaction models when predicting the random incidence absorption coefficient of finite porous materials.

2. Theory

2.1. Random incidence absorption coefficient

The theoretical random incidence absorption coefficient for plane wave incidence on an infinitely large surface is calculated using Paris' law by [8, 9]

$$\alpha_{rand} = \int_0^{\pi/2} \alpha_{inf}(\theta_i)\sin(2\theta_i)\,d\theta_i, \tag{1}$$

where $\alpha_{inf}(\theta_i)$ is the oblique incidence absorption coefficient at the incidence angle θ_i. It assumes that the intensity of the incident sound is uniformly distributed over all possible directions, and the phases of the incident waves on the absorber are randomly distributed. Large discrepancies between the theoretical random incidence absorption coefficient and the measured Sabine absorption coefficient are found throughout the entire frequency range of interest [10, 11], mainly due to non-uniform sound intensity on absorbers [12] and finite specimens [13].

2.2. Size corrected absorption coefficient

This section aims to theoretically compare the formulation by Thomasson [6] and Atalla et al. [4] for predicting the random incidence absorption coefficient of finite porous materials. As we shall see, both methods lead to the same formulation, but the approach is fundamentally different. Thomasson [6] makes use of a variational approach to derive the radiation impedance of a finite size specimen (Rayleigh-integral based) and simple formulas for the area correction of the absorption coefficient. Instead, Atalla et al. [4] directly solve the Rayleigh-integral. The idea behind their approach is to replace the infinite size radiation impedance in the receiving medium by the radiation impedance of an equivalent baffled window.

2.2.1. Thomasson's original model

Using a variational approach, Thomasson derived a size correction for the random incidence absorption coefficient by considering the average radiation (or field) impedance for a finite size at an oblique angle of incidence as follows [6]

$$\alpha_{size} = 2\int_0^{\pi/2} \frac{4Re(Z_s)}{|Z_s + \overline{Z_r}(\theta_i)|^2}\sin(\theta_i)d\theta_i, \tag{2}$$

where Z_s is the normal surface impedance of the test specimen, $\overline{Z_r}(\theta_i)$ is the averaged radiation impedance over azimuthal angles from 0 to 2π expressed as $\overline{Z_r}(\theta_i) = \int_0^{2\pi} Z_r(\theta_i)\,d\varphi/2\pi$ and φ is the azimuthal angle. $Z_r(\theta_i)$ is the radiation impedance, which is known to be $1/\cos(\theta_i)$ for an infinitely large plate. The radiation impedance for a finite panel is expressed as follows [6]

$$Z_r(\theta_i) = \frac{jk}{S} \iint \iint G(M, M_0) e^{jk\left(\mu_x(x_0-x)+\mu_y(y_0-y)\right)} dx dy dx_0 dy_0, \quad (3)$$

where k is the wavenumber, $S = \iint dxdy$, $\mu_x = \sin(\theta_i)\cos(\varphi)$, $\mu_y = \sin(\theta_i)\sin(\varphi)$, $G = (2\pi R)^{-1} e^{jkR}$ and $R = \sqrt{(x - x_0)^2 + (y - y_0)^2}$.

Note that here e^{jwt} is assumed, while Thomasson originally used a negative time convention. The calculation of the average radiation impedance requires numerical integration. Alternatively, one can refer to [6] where $\overline{Z_r}(\theta_i)$ is included for some common shapes. Averaging the radiation impedance over azimuthal angles is a suitable approximation when trying to reduce the calculation cost.

2.2.2. Finite transfer matrix method (FTMM)

To take into account the effect of the finite size, Atalla et al. [4] suggested a method that makes direct use of the Rayleigh-integral in connection with the transfer matrix method for calculation of the surface impedance of the material under test. The idea behind the approach is to replace the infinite size radiation impedance in the receiving medium by the radiation impedance of an equivalent baffled window. The size corrected random incidence absorption coefficient is then given by

$$\alpha(\theta_i, \varphi) = \frac{1}{\cos(\theta_i)} \frac{4Re(Z_s(\theta_i, \varphi))}{|Z_s(\theta_i, \varphi) + Z_r(\theta_i, \varphi)|^2}, \quad (4)$$

where Z_s is the normal surface impedance of the test specimen. The “baffled” radiation impedance introduced by Atalla et al. [4] is the same radiation impedance as the one defined earlier by Thomasson except for the opposite time convention. An analytical simplification of the FTMM has later been suggested by Rhazi et al. [5] that allows for a faster computation of the radiated power of multilayered materials. This FTMM version will be examined in the following.
It can be observed that for infinitely large specimens, that is when replacing the “baffled” radiation impedance by the inverse of the cosine, equation (4) becomes

$$\alpha_{inf}(\theta_i) = \frac{4Re(\zeta)\cos(\theta_i)}{|\zeta|^2\cos^2(\theta_i) + 2Re(\zeta)\cos(\theta_i) + 1}$$
$$= 1 - \left| \frac{\zeta - \frac{1}{\cos(\theta)}}{\zeta + \frac{1}{\cos(\theta)}} \right|^2, \quad (5)$$

where ζ is the specific surface impedance $Z_s/\rho_0 c_0$, with ρ_0 the air density and c_0 the speed of sound in air. It is worth underlining that replacing $1/\cos(\theta)$ in equation (5) by the “baffled” radiation impedance is not strictly correct.
Paris’ law applied to equation (4) leads to the exact same formulation of the size corrected random incidence absorption coefficient than equation (2). Differences lie in the approach and in the averaged radiation impedance over azimuthal angles used in Thomasson’s formulation. It should also be noted that both formulations assume the absorbing specimen to be flush-mounted in an infinite baffle, which differs from most practical application.

2.3. Local vs. extended reaction model

Regardless of the formalism, the surface impedance of the material can be calculated according to the transfer matrix method (TMM), which has been thoroughly described in [14]. When calculating the surface impedance, the simplest surface reaction model is referred to as *locally reacting* and assumes that the wave transmitted into a porous material is refracted so that it propagates effectively only perpendicular to the surface [15]. In other words, the surface impedance does not change with the angle of incidence. However, *extended reaction* is considered physically more correct, in particular for porous materials backed by an air-cavity. When extended reaction is assumed instead, Snell’s law determines the angle of transmission and waves are no longer transmitted in the perpendicular direction to the surface of interest. For absorbers with an air gap, large differences between the two reaction models are found, since the surface impedance at oblique incidence is noticeably different from the normal incidence surface impedance [7]. Assuming extended reaction, the size corrected random incidence absorption coefficient can be expressed as

$$\alpha_{size} = 2 \int_0^{\pi/2} \frac{4Re(Z_s(\theta_i))}{|Z_s(\theta_i) + \overline{Z_r}(\theta_i)|^2} \sin(\theta_i) d\theta_i. \quad (6)$$

If using the averaged radiation impedance over azimuthal angles. It should be noticed that Thomasson originally assumed local reaction. A similar variational approach has recently been used by Brunskog [16], who showed that, for the forced sound transmission of a finite wall, the use of extended reaction results in the same formulation. This also holds for the case of absorption of finite patches, resulting in equation (6).

3. Method

In the following, the FTMM is systematically compared to Thomasson's model assuming extended reaction. It can be anticipated from the theoretical section that a good agreement between the results will be found. The two surface reaction models will be examined using Thomasson's formulation. The simulations are conducted on "known" specimens for experimental comparison, and denoted as **Specimen 1** and **Specimen 2** respectively:

(1) 100 mm Rockwool (flow resistivity 19.8 kPa.s.m^{-2}) with rigid backing;

(2) 100 mm Glass wool (flow resistivity 12.8 kPa.s.m^{-2}) with a 100 mm air-cavity backing.

The absorption of the first specimen has been measured according to ISO 354 in a round robin test including 13 European reverberation chambers [17]. The second specimen is referred to as the "reference absorber" and has been suggested in previous studies to calibrate the reverberation chambers for absorption coefficient measurements [18]. The reference absorber is measured in an ongoing round robin test, which includes so far 7 European reverberation chambers (part of the results has been published in [18]). The acoustical properties of both porous materials are modelled using Delany-Bazley's empirical model [19] or alternatively its modification by Miki [20]. Both require the flow resistivity as the only parameter.

4. Results and analysis

Figures 1 and **2** show the simulation results for Specimen 1 and Specimen 2 respectively. The FTMM is compared to Thomasson's model under extended reaction assumption. Thomasson's results are displayed for both local and extended reaction assumptions. The respective round robin mean results are superimposed for comparison.

A good agreement is found in both cases between the FTMM and Thomasson's model. The small deviations might be explained by the use of the average radiation impedance over azimuthal angles in Thomasson's formulation. In the case of a rigid backing, the two surface reaction models yield equivalent results. Large discrepancies are however found in the low-frequency range in the case of a backing cavity. Extended reaction is best suited to the cavity case and should systematically be used regardless of the configuration (with or without cavity backing). The results based on extended reaction only will be discussed in the following.

The simulation results are overestimating the measured absorption in the low frequency range, by up to 25% for the rigid backing condition and by up to 65% in the presence of a cavity. The following discussion aims to give an overview of the possible explanations for such a disagreement between simulation results and measured data. However, this paper has no intention to give a complete survey. Additionally, a few suggestions are given to overcome the issue.

A straightforward explanation would be the lack of a diffuse sound field in the low frequency range in the measurement facilities. More precisely, the results reveal an unbalance between the sound intensities contained in the grazing sound field and the non-grazing sound field respectively. In other words, the intensity of the incident sound on the

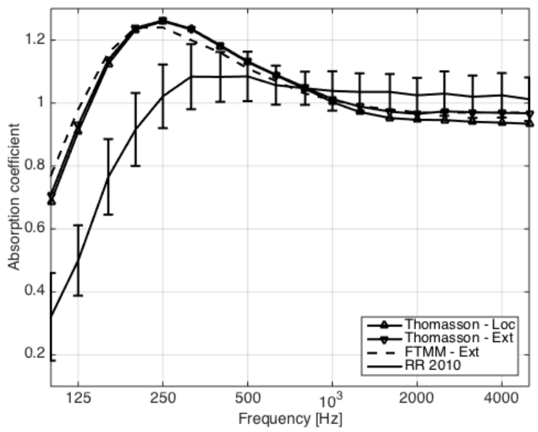

Figure 1 – Absorption coefficient of Specimen 1 - FTMM vs. Thomasson. Mean round robin test results superimposed. Area of the test specimen: 3 x 3.6 m

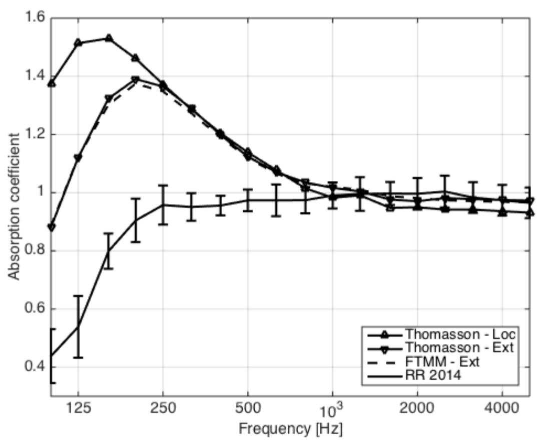

Figure 2 – Absorption coefficient of Specimen 2 - FTMM vs. Thomasson. Mean round robin test results superimposed. Area of the test specimen: 3 x 3.6 m

test specimen is not uniformly distributed over all possible directions unlike Paris' law (see equation (1)). An easy trick to avoid this problem is to place an upper limit on the angles of incidence in the integration associated with Paris' law. **Figure 3** shows the effect of truncating the integration angle to 78 degrees (this arbitrary truncation value is by no way a suggestion, but aims to provide a better understanding of the sound field behavior in the actual measurement situation). Using the truncation, the predicted absorption is lower in the low-frequency range and closer to the experimental data. This indicates that overall, in the test chambers, less sound intensity is contained in the grazing sound field than it does in theory. The grazing part of the sound field is most likely redirected into the non-grazing part via the diffusers installed in the chambers. The truncation method leads to results closer to the experimental data in that it artificially removes part of the contribution of the grazing sound field in the model. Still, the adjustment of the truncation angles remains uncertain.

Another solution is based on the modal decomposition method (MDM), as described by Schultz et al. [21], who resolved the sound field inside a rectangular duct. The method is here extended to the case of a plane-parallel space, which mimics the reverberation chamber, and considers a two-dimensional modal field in a plane parallel to the absorptive specimen. Schultz et al. [21] express the solution to the Helmholtz equation in a closed area as the summation of transverse modes. Hence for a two-dimensional modal field, the transverse wavenumber $k_t = k_0 \sin(\theta)$ is replace by

$$k_{mn} = \sqrt{\left(\frac{m\pi}{L_x}\right)^2 + \left(\frac{n\pi}{L_y}\right)^2}. \tag{7}$$

The incident angle θ_{mn} associated to the (m, n) mode is therefore

$$\theta_{mn} = \sin^{-1}\left(\frac{k_{mn}}{k_0}\right). \tag{8}$$

Modal decomposition involves the use of a discrete sum over the (m, n) modes so that equation (2) becomes

$$\alpha_{modal} = \frac{\sum_m \sum_n \alpha_{size}(\theta_{mn})}{\sum_m \sum_n \cos(\theta_{mn}) \sin(\theta_{mn})}, \tag{9}$$

which simply results in another way of integrating the incident sound field.

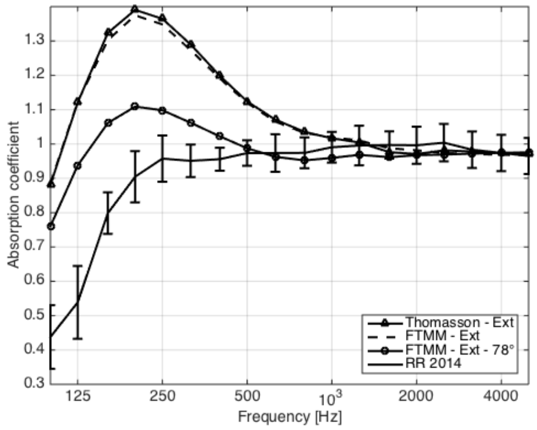

Figure 3 – Absorption coefficient of Specimen 2 – Truncation of the integration angle in FTMM. Mean round robin test results superimposed. Area of the test specimen: 3 x 3.6 m

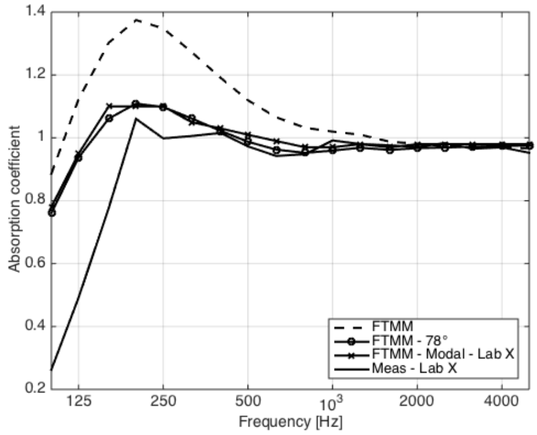

Figure 4 – Absorption coefficient of Specimen 2 – FTMM – diffuse field excitation vs. modal excitation. Measurement results in the chamber of concern superimposed. Area of the test specimen: 3 x 3.6 m

Figure 4 compares the size-corrected absorption coefficient estimated with the FTMM under modal excitation, the FTMM under diffuse field excitation and the FTMM under diffuse field excitation limited to an angle of incidence of 78°. The simulations are performed for 100 mm Glass wool with air-cavity backing. The modal decomposition method is here applied for a simple plane-parallel reverberation chamber (6.26 x 7.86 x 4.90 m), which took part in the ongoing round robin test. Limiting the integration angle to 78° is an empirical method which allows avoiding grazing waves. The modal decomposition method retrieves this method by using the actual dimensions of the room. However the model does not allow for detailed implementation of the geometry, including boundary or panel diffusers installed in the actual reverberation chamber. Discrepancies however remain between the measured and simulated data. A plausible explanation is that the model assumes the absorptive specimen to be flush-mounted in an infinite baffle. This is evidenced by the fact that the disagreement is larger in the case of the cavity, where the total height of the sample is increased. It is however not straightforward to predict the actual behavior of the sound field in the presence of such a discontinuity. Future work could examine the possibility of including the effect of the discontinuity within the available models. A more systematic analysis of the effect of flush mounting on measurement results would also be required.

5. Conclusions

The radiation impedance models suggested by Thomasson [6] and Rhazi et al. [5] have been compared when predicting the random incidence absorption coefficient of finite porous materials. The methods are found to yield comparable results and hold for extendedly reacting surfaces.
Discrepancies with measurement results can essentially be explained by the unbalance between grazing and non-grazing sound field in the reverberation chamber. Promising results are found when incorporating the modal decomposition method. Future work will examine the effect of the mounting of the test specimen in the reverberation chamber, which differs from the flush mounting in an infinite baffle as assumed in the models.

Acknowledgement

The authors would like to thank François-Xavier Bécot, Tor Erik Vigran and Gerd Høy Marbjerg for comments and discussion.

References

[1] L. Cremer and M. Heckl, Körperschall, Springer-Verlag, Berlin, 1967

[2] L. Cremer, M. Heckl and E. E. Ungar, Structure-Borne Sound, Springer-Verlag, Berlin, 1988

[3] M. Villot, C. Guigou and L. Gagliardini, Predicting the acoustical radiation of finite size multi-layered structures by applying spatial windowing on infinite structures, Journal of Sound and Vibration (2001) 245(3), 433-455

[4] N. Atalla, F. Sgard and C. Kafui-Amedin, On the modelling of sound radiation from poroelastic materials, J. Acoust. Soc. Am. 120(4), pp. 1990-1996, October 2006

[5] D. Rhazi and N. Atalla, A simple method to account for the size effects in the transfer matrix method, Journal of Sound and Vibration 127 (2), February 2010

[6] S.I. Thomasson, On the absorption coefficient, Acustica 44, 265-273 (1980)

[7] C.H. Jeong, Guideline for adopting the local reaction assumption for porous absorbers in terms of random incidence absorption coefficients, Acta Acustica, Vol 97 779-790 (2011)

[8] H. Kuttruff, Room Acoustics, Fifth Edition, 2009

[9] E.T. Paris, On the reflexion of sound from a porous surface, Proc Roy Soc 115, pp. 407-419 (1927)

[10] C.W. Kosten, International comparison measurement in the reverberation room, Acustica 10, 400-411 (1960)

[11] C.H. Jeong, Non-uniform sound intensity distributions when measuring absorption coefficients in reverberation chambers using a phased beam tracing, J. Acoust. Soc. Am. 127, 3560–3568 (2010)

[12] C.H. Jeong, A correction of random incidence absorption coefficients for the angular distribution of acoustic energy under measurement conditions, J. Acoust. Soc. Am. 125, 2064–2071 (2009)

[13] R.K. Cook, Absorption of sound by patches of absorbent material, J. Acoust. Soc. Am. 29, 324–329 (1957)

[14] B. Brouard, D. Lafarge and J. F. Allard, A general method of modelling sound propagation in layered media, Journal of Sound and Vibration (1995) 183(1), 129-142

[15] K. Attenborough, Acoustical characteristics of porous materials, Phys. Rep. 82, 179-227 (1982)

[16] J. Brunskog, The forced sound transmission of finite single leaf walls using a variational technique, J. Acoust. Soc. Am. 132 (3), September 2012

[17] M.L.S. Vercammen, Improving the accuracy of sound absorption measurement according to ISO 354, Proceedings of the International Symposium on Room Acoustics, Melbourne, Australia, 2010

[18] M. Nolan, M. Vercammen, C.H. Jeong and J. Brunskog, The use of a reference absorber for absorption measurements in a reverberation chamber, Proceedings of Forum Acusticum 2014, Krakow, Poland, 2014

[19] M.E. Delany and E.N. Bazley, Acoustical properties of fibrous absorbent materials, Appl. Acoust. 3, 105-116 (1970)

[20] Y. Miki, Acoustical properties of porous materials – modifications of Delany-Bazley models, J. Acoust. Soc. Jpn. 11, 19–28 (1990)

[21] T. Schultz, L.N. Cattafesta III and M. Sheplak, Modal decomposition method for acoustic impedance testing in square ducts, J. Acoust. Soc. Am. 120(6), 3750–3758 (2006)